Mapana - Journal of Sciences
2023, Vol. 22, No. 3, *165-190*
ISSN 0975-3303 | https://doi.org/10.12723/mjs.66.10

Weakly non-linear stability of Maxwell Fluid in a Porous Layer with the effect of Magnetic field

C. Bheemudu*, T. Ramakrishna Goud†

Abstract

The problem of magnetoconvection over a Maxwell fluid due to porous media with the Darcy–Brinkman model via magnetic field is studied. Analytical results of the critical Darcy–Rayleigh numbers at the onset of stationary convection and oscillatory convection are derived. The governing dimensionless equations are tackled through the normal mode approach, resulting in an eigenvalue problem within the context of linear stability theory.

Furthermore, we harness the power of the Galerkin first-order method in MATLAB R2020a to address and resolve this eigenvalue problem. The behavior of various parameters, like the Q,Λ,Da, and Pm, has been analyzed. The neutral curves are obtained for different prescribed values of the other physical parameters. The Chandrasekhar and Darcy numbers stabilize the system, and the Critical oscillatory Rayleigh number is a non-monotonic function of Pm. In order to study the heat

* Department of Mathematics, Osmania University, Telangana, India, 500007; Email: bheemuduc938@gmail.com

transport by convection, the well-known Ginzburg-Landau equation has been derived using weakly non-linear analysis.

Keywords: Maxwell fluid, Magnetic effect, Porous media, Convection.

1. Introduction

In the geological context, double-diffusive convection processes in the sedimentary basin evolution, metamorphism, crustal heat and solute transport, and ore genesis. In the hydrogeological processes, mixed convection in porous media possesses the lower-level transposition of nuclear wastes, liquid reinjection, transport of over-saturated soil, electro-chemical processes, and the migration in fibrous insulation. A porous medium is a material or substance characterized by interconnected voids, pores, or cavities that facilitate the passage of fluids, including liquids and gases. These pores exhibit a diversity of sizes and shapes, and their arrangement within the medium has a notable impact on fluid flow characteristics. Both mathematical models and experimental techniques are employed to explore fluid behavior within porous media, bearing significant consequences for a range of practical applications and environmental concerns. An early double-diffusive convective instability problem was studied in a horizontal salted layer heated from below and later studied with the porous media by Nield [5] at different solutal and thermal boundary conditions. He identified overstability when stabilizing solute inclines and possible salt fingers are tapered in a porous medium. Later this was extended by Taunton et al. [6], Rudraiah et al. [8], and others. Poulikakos [9] studied the linear stability analysis of the double-diffusive convection by using the Darcy-Brinkman model. Malashetty [11] investigated the linerar stability of the diffusive equilibrium in a horizontal plane porous layer of a binary mixture of two miscible fluids. Kalla et al. [12] studied multiple convective cases analytically and numerically when the horizontal porous layer is heated below within mixed fluids. The model of double-diffusive convection in a porous medium has been extensively investigated by Ingham and Pop [13], Nield and Bejan [17], Vadasz [22], Benerji et al. [26, 27], and Reddy et al [28].

Darcy postulated the empirical relation when fluid flow through the porous media is directly proportional to the pressure gradient and this is known as the Darcy model. The below eq. (1) relation inserted in the momentum equation, which is

$$\mathbf{q} = -\frac{K}{\mu}\left(\nabla p - \rho g\right). \tag{1}$$

Where the permeability of a porous medium is K. The modified Darcy law was including the local acceleration term and this is known as the modified Darcy model or Darcy-Lapwood model and the relation eq. (2) is

$$\frac{\partial \mathbf{q}}{\partial t} = -\frac{\epsilon}{\rho}\left(\nabla p - \rho g + \frac{\mu}{K}\mathbf{q}\right). \tag{2}$$

In anisotropic, it is in the form of

$$\frac{\partial \mathbf{q}}{\partial t} = -\frac{\epsilon}{\rho}\left(\nabla p - \rho g + \mu K.\mathbf{q}\right). \tag{3}$$

When the flow is curvilinear and the curvature of the path through porous media then the inertia effect, becomes, the streamlines are distorted more and the drag increases more rapidly. In this situation the relation eq. (3) becomes added with the inertial term (q. Δ)q, this was referred to by Lapwood

$$(\mathbf{q} \cdot \nabla)\, \mathbf{q} = -\epsilon^2 \left(\nabla p - \rho g + \frac{\mu}{K} \mathbf{q} \right). \tag{4}$$

If the pattern of fluid is unsteady in a certain region then considered the local acceleration term $\frac{1}{\epsilon} \frac{\partial \mathbf{Q}}{\partial t}$ and it is known as the modified Darcy-Lapwood model or Darcy-Lapwood-Brinkmann model, the relation is

$$\rho \left[\frac{1}{\epsilon} \frac{\partial \mathbf{q}}{\partial t} + \frac{1}{\epsilon^2} (\mathbf{q} \cdot \nabla)\, \mathbf{q} \right] = - \left(\nabla p - \rho g + \frac{\mu}{K} \mathbf{q} \right). \tag{5}$$

Maxwell's model [10] is the widely used first viscoelastic rate type model in gases but it is not a model for storing energy fluids and dissipation energy fluids. Maxwell makes an equivalence with the constitutive equation of the Maxwell fluid due to a porous medium. Khuzhayorov et al. [15] investigated the Non-Newtonian fluids due to porous medium and generalized dynamically permeable Darcy's law used for porous medium. This system is valid at small Reynolds and Deborah numbers. The momentum equation in the modified Darcy–Maxwell model involved the equation (6), given below

$$\left(1 + \overline{\lambda} \frac{\partial}{\partial t} \right) \nabla P = -\frac{\mu}{K} V. \tag{6}$$

Hayat et al. [19]-[20] developed Homotopy Analysis Method to analyze the magnetohydrodynamic flow of a Maxwell fluid via porous through suction and injection stretching sheet and studied the convergence of the series, skin friction, local Nusselt number, and velocity. Abbas et al. [18] investigated the Maxwell fluid porous channel using the homotopy analysis method and the effects were studied with Deborah number De, Reynolds number Re, and Hartmann number M parameters for suction and injection. Wang and Tan [24] investigate the modified Darcy-Maxwell model at the onset of stability analysis for viscoelastic fluid with the Soret effect. Here, the Soret effect destabilizes the oscillatory convection, and relaxation time enhances the instability. The variation of the Rayleigh number with respect to the Nusselt number was derived at the modes of stationary and oscillatory. Malashetty and Biradar [25] analyzed Maxwell fluid's linear and nonlinear instabilities in a saturated porous medium by using the Darcy-Maxwell method in the momentum equation. Gaikwad and Dhanraj [21] scrutinized the effects of anisotropic and internal heating on the binary Maxwell liquid in a permeable layer. Raghunatha et al. [29] investigated the instabilities of the diffusive convection in a Maxwell fluid via a porous medium which was derived from the Darcy model. Their exits oscillatory neutral curves indicate the Darcy Rayleigh number versus wave number. Observed quasi-periodic bifurcation at the rest of the state and point out the bifurcation is either critical, sub-critical, or super-critical depending on the physical parameters. Karimi et al.[30], Rastegarpouyani et al.[31] investigated biosamples with machine learning approaches and mono-infection, co-infections. Hosseinzadeh et al. [32] used a 2DDarcy-Forchheimer model for porous medium and used numerical methods to demonstrate the system. He evaluated and observed the Nusselt number, Eckert number, and temperature to study the model. The Application of numerical methods was investigated by Jahanmahin et al.[33], Pasha et al. [34] , Fathollahi et al.[35], and Faress et al.[36]. Recently Charchi et al.[37], Abdollahzadeh et al.[38], and Shadman et al.[42] examined the film-coupled nanostar resonators, hybrid nanofluids with nanotubes, and Magnetic nanofluids with a stretching sheet respectively. Reddy and Ravi [39] studied the states of perturbed states with small amplitude using the eigenvalue problem at the onset of convection for Maxwell fluid with porous. They studied quantities of various parameters at stationary and oscillatory and found that the Damkohler number has a contrast effect on steady and oscillatory convection.

The magnetic field has significant applications in various contents like material processing, liquid metals convection, steel casting systems, electric Motors, electromagnets, electric generators, electromagnetic wave propagation, thermal wind tunnel, and other contents. Alfven [1] first studied the interrelation between the magnetic field with electrically conducting fluid over a solar field. Thompson [2]produced the Jefferey's theory over convection with the effect of magnetic field for non-viscous fluids and discussed the oscillations. He added ponderomotive force jX**H** in the momentum equation, where **H** is the magnetic field and j is the current density. The current density j is

$$\mathrm{j} = \rho\left(\mathbf{E} + \mu\frac{\mathbf{V}}{c}X\mathrm{H}\right). \tag{7}$$

In this, the fields satisfy Maxwell's equations. Sparrow and Cess [4] studied the onset of convection due to buoyancy and magnetic forces over vertical plates and found magnetic field should show a significant effect at the time of convection in liquid metals compared with fluids. Knobloch et al [7] present the convection in Boussinesq fluid due to a magnetic field, the diffusivity ratio of the magnetic field over the thermal field is small when the magnetic field is large. The model is static equilibrium when $R = R_e < R_o$ and there exists a steady solution for $R > R_c$ and unstable for $R_e < R < R_c$ and there exists Hopf bifurcation at R = Rc.. Where R represents the Rayleigh number and suffix e, o and c represents equilibrium, over stable and critical respectively. Uetake et al. [14], Sharma [16], Ghosh [23], Ravi and Suman [40], and Benerji et al. [41] studied the effect ofthe magnetic field over different fluids at variant boundaries with other conditions.

From the literature, it is clear that the problem of magnetoconvection of a Maxwell fluid in a porous layer has not been studied yet. In the present analysis, we aim to fill this research gap by conducting both linear and weakly non-linear stability analyses of a Maxwell fluid flowing through a porous layer while considering the influence of a magnetic field. By examining the linear and weakly non-linear stability characteristics, we aim to gain deeper insights into the magnetoconvection phenomenon and the behavior of Maxwell fluids in porous media under the influence of a magnetic field. Section 2 describes the mathematical model of the problem. In Sect. 3, we derive the Rayleigh number and its critical value at the stationary and oscillatory stages. In Sect. 4, we obtain the two-dimensional amplitude equation. Finally, we present the results and discussions in Sect. 5 through graphical images and tabular data.

2. Basic Equations

Let us assume a horizontal layer of Maxwell fluid heated from below confined between $z\varepsilon(0, d)$ with constant temperature θ_0 and $\theta_0 + \Delta\theta(\Delta\theta > 0)$ are maintained at upper and lower boundaries, respectively, and gravity force g acts on it. Then, according to [26], [32], [39], the governing equations with the Boussinesq approximation are

$$\nabla \cdot V = 0, \nabla \cdot H = 0, \tag{8}$$

$$\left(1 + \overline{\lambda}\frac{\partial}{\partial t}\right)(\nabla P - \rho g) + \frac{\mu}{\kappa}V - \mu_e \nabla^2 V + \frac{\mu_m}{\rho_0}(\nabla \times H) \times H = 0, \tag{9}$$

$$\frac{\partial \theta}{\partial t} + (V \cdot \nabla)\theta = k\nabla^2\theta, \tag{10}$$

$$\epsilon\frac{\partial H}{\partial t} + (V \cdot \nabla) H - (H \cdot \nabla) V = \eta \nabla^2 H, \tag{11}$$

$$\rho = \rho_0 \left[1 - \alpha(\theta - \theta_0)\right], \tag{12}$$

along with the boundary conditions

$$\begin{array}{llll} at \quad z = 0 : & V = 0 & \theta = \theta_0 + \Delta\theta & H = H_0, \\ at \quad z = d : & V = 0 & \theta = \theta_0 & H = H_0. \end{array} \tag{13}$$

The basic state of the Maxwell fluid is derived as

$$V_b = 0,\ \rho = \rho_b(z),\ \theta_b = \theta_0 - \left(\frac{\Delta\theta}{d}\right)z,\ H_b = \overline{e_z}. \tag{14}$$

The model defined by Eqs. (8)-(11) is non-dimensionalised by choosing the transformations

$$\begin{aligned} (x^*, y^*, z^*) &= \left(\frac{x}{d}, \frac{y}{d}, \frac{z}{d}\right), \\ (u^*, v^*, w^*) &= \left(\frac{d}{k}u, \frac{d}{k}v, \frac{d}{k}w\right), \\ (t^*, H^*, \theta^*) &= \left(\frac{k}{d^2}t, \frac{H}{H_0}, \frac{\theta}{\Delta\theta}\right). \end{aligned} \tag{15}$$

By using non dimensional quantities from Eq 15 non dimensionalize the Eqs. (8)-(11) on dropping the asterisks for simplicity, the dimensionalized equations are

$$\nabla \cdot V = 0, \nabla \cdot H = 0, \tag{16}$$

$$\left(1 + \overline{\lambda}\frac{\partial}{\partial t}\right)(\nabla P - R\theta\overline{e_z}) + V - Da\nabla^2 V + QPm(\nabla \times H) \times H = 0, \tag{17}$$

$$\frac{\partial \theta}{\partial t} + (V \cdot \nabla)\theta = w + \nabla^2\theta, \tag{18}$$

$$\frac{\partial H}{\partial t} + (V \cdot \nabla) H - (H \cdot \nabla) V = \frac{\partial w'}{\partial z} + Pm\nabla^2 H, \tag{19}$$

and along with the boundary conditions

$$\begin{aligned} at \quad z=0 \ : \quad & V=0, \quad \theta=1 \quad and \quad H=\overline{e_z}, \\ at \quad z=1 \ : \quad & V=0, \quad \theta=0 \quad and \quad H=\overline{e_z}. \end{aligned} \tag{20}$$

The controlling parameters are the thermal Rayleigh number (R), Darcy number (Da), Chandrasekhar number (Q), Magnetic Prandtl number (Pm) and Deborah number (λ) are given by

$$R=\frac{g\Delta T\kappa d\rho_0\alpha}{\mu k},\ Da=\frac{\mu_e}{\mu},\ Q=\frac{\mu_m H_o^2\kappa}{\mu\rho_0\eta},\ \lambda=\frac{\overline{\lambda}k}{d^2},\ Pm=\frac{\eta}{k}. \tag{21}$$

All quantities which are used in the above equations have been explained in nomenclature.

Take the z- component of curl of curl eq. (17) and the third component of eq.(19), we get

$$\left(1+\lambda\frac{\partial}{\partial t}\right)R\Delta_h^2T-\nabla^2w+Da\nabla^4w+QPm\nabla^2\frac{\partial H_z}{\partial z}=0, \tag{22}$$

$$\frac{\partial H_z}{\partial t}-\frac{\partial w}{\partial z}=Pm\nabla^2H_z, \tag{23}$$

$$\frac{\partial\theta}{\partial t}-w=\nabla^2\theta, \tag{24}$$

and along with the boundary conditions

$$\begin{aligned} at\ z=0 \ : \quad & w=0, \quad \theta=0, \quad and \quad \frac{\partial H_z}{\partial z}=0, \\ at\ z=1 \ : \quad & w=0, \quad \theta=0, \quad and \quad \frac{\partial H_z}{\partial z}=0. \end{aligned} \tag{25}$$

Where $\nabla^2=\frac{\partial^2}{\partial x^2}+\frac{\partial^2}{\partial y^2}+\frac{\partial^2}{\partial z^2}$ and $\nabla_h^2=\frac{\partial^2}{\partial x^2}+\frac{\partial^2}{\partial y^2}$. Now eliminating θ and H_z from eq.(22)-(24), one obtains

$$\mathcal{L}w=\mathcal{N}. \tag{26}$$

$$\begin{aligned} \mathcal{L}=QPm\nabla^2\frac{\partial^2}{\partial z^2}\left(\frac{\partial}{\partial t}-\nabla^2\right)+\left(\frac{\partial}{\partial t}-Pm\nabla^2\right)\left(1+\lambda\frac{\partial}{\partial t}\right) \\ +\nabla^2\left(Da\nabla^2-1\right)\left(\frac{\partial}{\partial t}-\nabla^2\right)\left(\frac{\partial}{\partial t}-Pm\nabla^2\right), \end{aligned} \tag{27}$$

$$\mathcal{N}=\left(\frac{\partial}{\partial t}-Pm\nabla^2\right)\left(1+\lambda\frac{\partial}{\partial t}\right)(V.\nabla)\theta+QPm\left(\frac{\partial}{\partial t}-Pm\nabla^2\right)\left((H\cdot\nabla)V-(V\cdot\nabla)H\right). \tag{28}$$

3. Linear stability analysis Let us substitute $w = \sin \pi z e^{i(lx+my)+pt}$ [3] and [39], in the linear form of eq. (26) and hence Lw = 0, hence one obtains

$$a_0\delta^8 + a_1\delta^6 + a_2\delta^4 + a_3\delta^2 + a_4 = 0, \quad (29)$$

where

$$\begin{aligned} a_0 &= DaPm, \quad (30)\\ a_1 &= (Pm + Da\sigma),\\ a_2 &= Da\sigma^2 + \sigma(1 + Pm\pi^2 PmQ),\\ a_3 &= \sigma^2 + \pi^2 PmQ\sigma - Pmq^2R(1+\lambda\sigma),\\ a_4 &= Rq^2\sigma(1+\lambda\sigma). \end{aligned}$$

3.1. Stationary instability First, we consider stationary instability, i.e., $\sigma = 0$ is real. The stationary Rayleigh number R_s can be written as

$$R_s = \frac{\pi^2 Q\delta^2 + \delta^4 + Da\delta^6}{q^2}. \quad (31)$$

3.2. Oscillatory instability To study the oscillatory stability, consider the both real and imaginary parts of Rayleigh number R. The Rayleigh number at the onset of oscillatory convection is

$$R = R_r + iR_i, \quad (32)$$

where *Rr* and *Ri* are real and imaginary part of Rayleigh number.

$$R_r = \frac{(1+Da\delta^2)(\omega^2 + Pm^2\delta^4)(\delta^2+\omega^2\lambda)\delta^2 + \pi^2\delta^2 QPm\left[Pm\delta^4 + \omega^2 + (-1+Pm)\lambda\delta^2\omega^2\right]}{q^2(\omega^2+Pm^2\delta^4)(1+\omega^2\lambda^2)}, \quad (33)$$

$$R_i = \frac{(1+Da\delta^2)(\omega^2 + Pm^2\delta^4)\omega\lambda^2 - \omega^2\delta^2\lambda\left[n^2\pi^2 PmQ(\omega^2+Pm\delta^4) + \delta^2(1+Da\delta^2)(\omega^2 + P\right.}{q^2(\omega^2+Pm^2\delta^4)(1+\omega^2\lambda^2)} \quad (34)$$

$$\omega^2 = \frac{Pm^2\delta^4(1+Da\delta^2)(-1+\delta^2\lambda) + Pm\pi^2\delta^2 Q\left[1 + Pm(-1+\delta^2\lambda)\right]}{1 - \pi^2 PmQ\lambda - \delta^2\lambda + Da\delta^2(1-\delta^2\lambda)}, \quad (35)$$

$$R_o = \frac{\pi^4 Pm^2 Q^6\delta^6(-1+Pm)^2(-1+\delta^2\lambda)^2 A^2 + (1+Pm\lambda\delta^2)^3 B^2}{q^2 B^4}, \quad (36)$$

where the values of *A* and *B* are

$$\begin{aligned} A &= QPm\pi.^2\left(1+Da\delta^2\right)(1+Pm)\delta^2, \quad (37)\\ B &= -1 + \pi^2 PmQ\lambda + \lambda\delta^2 + Da\delta^2\left(-1+\delta^2\lambda\right). \end{aligned}$$

4. Weakly non linear analysis Let us introduce the following series expansion interms of e

$$\begin{aligned}
u &= \epsilon u_0 + \epsilon^2 u_1 + \epsilon^3 u_2 + \cdots ,\\
v &= \epsilon v_0 + \epsilon^2 v_1 + \epsilon^3 v_2 + \cdots ,\\
w &= \epsilon w_0 + \epsilon^2 w_1 + \epsilon^3 w_2 + \cdots ,\\
\theta &= \epsilon \theta_0 + \epsilon^2 \theta_1 + \epsilon^3 \theta_2 + \cdots ,\\
H_x &= \epsilon H_{x_0} + \epsilon^2 H_{x_1} + \epsilon^3 H_{x_2} + \cdots ,\\
H_y &= \epsilon H_{y_0} + \epsilon^2 H_{y_1} + \epsilon^3 H_{y_2} + \cdots ,\\
H_z &= \epsilon H_{z_0} + \epsilon^2 H_{z_1} + \epsilon^3 H_{z_2} + \cdots ,
\end{aligned} \tag{38}$$

where

$$\epsilon^2 = \frac{R - R_{sc}}{R_{sc}} << 1.$$

The first approximations are

$$\begin{aligned}
u_0 =& \frac{i\pi}{l_{sc}}\Big[Ae^{i(l_{sc}x+m_{sc}y)}\cos\pi z - c.c\Big],\\
w_0 =& \Big[Ae^{i(l_{sc}x+m_{sc}y)}\sin\pi z + c.c\Big],\\
H_{x_0} =& \frac{-i\pi^2}{l_{sc}Pm\delta_{sc}^2}\Big[Ae^{i(l_{sc}x+m_{sc}y)}\sin\pi z - c.c\Big],\\
H_{y_0} =& 0,\\
H_{z_0} =& \frac{\pi}{Pm\delta_{sc}^2}\Big[Ae^{i(l_{sc}x+m_{sc}y)}\cos\pi z + c.c\Big],\\
\theta_0 =& \frac{1}{\delta_{sc}^2}\Big[Ae^{i(l_{sc}x+m_{sc}y)}\sin\pi z + c.c\Big],
\end{aligned} \tag{39}$$

where the amplitude, A, is a function of slow variables X, Y,Z and T and the complex conjugate is denoted by c.c..The slow variables can be scaled as

$$X = \epsilon x, \quad Y = \epsilon^{\frac{1}{2}} y, \quad Z = z, \quad T = \epsilon^2 t,$$

Using the above scaling differential operators can be written as

$$\frac{\partial}{\partial x} + \epsilon\frac{\partial}{\partial X}, \quad \frac{\partial}{\partial y} \to \frac{\partial}{\partial y} + \epsilon^{\frac{1}{2}}\frac{\partial}{\partial Y}, \quad \frac{\partial}{\partial z} \to \frac{\partial}{\partial Z}, \quad \frac{\partial}{\partial t} \to \epsilon^2\frac{\partial}{\partial T}. \tag{40}$$

By using Eq. (40), the operators L and N of Eq. (26) can be written as

$$\begin{aligned}
\mathcal{L} =& \mathcal{L}_0 + \epsilon\mathcal{L}_1 + \epsilon^2\mathcal{L}_2 \cdots ,\\
\mathcal{N} =& \mathcal{N}_0 + \epsilon\mathcal{N}_1 + \epsilon^2\mathcal{N}_2 \cdots .
\end{aligned} \tag{41}$$

On substituting Eq. (41) into Eq. (26), and comparing the coefficients of ϵ, ϵ^2 and ϵ^3, one obtains

$$\mathcal{L}_0 w_0 = 0, \tag{42}$$

$$\mathcal{L}_0 w_1 + \mathcal{L}_1 w_0 = \mathcal{N}_0, \tag{43}$$

$$\mathcal{L}_0 w_2 + \mathcal{L}_1 w_1 + \mathcal{L}_2 w_0 = \mathcal{N}_1, \tag{44}$$

where

$$\mathcal{L}_0 = Pm\nabla^4 \left(-\nabla^2 + Da\nabla^4 - QD^2 - R_{sc}\left(1 + \lambda \frac{\partial}{\partial \tau}\right)\right), \tag{45}$$

$$\mathcal{L}_1 = 2\frac{\partial^2}{\partial x \partial X}\nabla^2 Pm \left(-3\nabla^2 + 4Da\nabla^4 - 2QD^2 - R_{sc}\left(1 + \lambda \frac{\partial}{\partial \tau}\right)\right), \tag{46}$$

$$\begin{aligned}\mathcal{L}_2 = & \frac{\partial^2}{\partial X^2}\left(4DaPm\nabla^6 - 3Pm\nabla^4 - 2QPmD^2\nabla^2 - PmR_{sc}\nabla^2\right) \\ & + \frac{\partial}{\partial \tau}\left(\nabla^4 - Da\nabla^6 + Pm\nabla^4 - DaPm\nabla^6 + QPmD^2\nabla^2 + R_{sc}\nabla^2\right) \\ & + \left(2\frac{\partial^2}{\partial x \partial X}\right)^2 \mathcal{F}_2\left(-3Pm\nabla^2 + 6DaPm\nabla^4 - QPmD^2\right) + \frac{\partial^2}{\partial \tau^2}\lambda R_{sc}\nabla^2. \end{aligned} \tag{47}$$

Let us Substitute the solution w_0 in to $\mathcal{L}_0 w_0 = 0.$. One obtains

$$R_{sc} = \frac{\pi^2 Q\delta_{sc}^2 + \delta_{sc}^4 + Da\delta_{sc}^6}{q_{sc}^2} \tag{48}$$

from the equation $\mathcal{L}_0 w_1 + \mathcal{L}_1 w_0 = \mathcal{N}_0, \mathcal{N}_, = 0$ and $\mathcal{L} w_0 = 0.$ The equation reduces to $w_1 = 0$,which implies $u_1 = 0$. Similarly, the first order solutions are

$$\begin{aligned} H_{x_1} &= 0, \\ H_{y_1} &= 0, \\ H_{z_1} &= \frac{\pi^2}{2Pml_{sc}\delta_{sc}^2\pi}\left[A^2 e^{2i(l_{sc}x + m_{sc}y)} + c.c\right], \\ \theta_1 &= -\frac{1}{2\pi\delta_{sc}^2\pi}|A|^2 \sin 2\pi z. \end{aligned} \tag{49}$$

On substituting the first order solutions into the Eq. (44), we obtain Newell-Whitehead equation in the form of

$$\lambda_0 \frac{\partial A}{\partial T} - \lambda_1 \left(\frac{\partial}{\partial X} - \frac{i}{2q_{sc}}\frac{\partial^2}{\partial Y^2}\right)^2 A - \lambda_2 A + \lambda_3 |A|^2 A = 0 \tag{50}$$

where

$$\begin{aligned} \lambda_0 &= (1 + Pm)Da\delta_{sc}^6 + (1 + Pm)\delta_{sc}^4 + \delta_{sc}^2\left(QPm\pi^2 - R_{sc}\right), \\ \lambda_1 &= Pm\left(3\delta_{sc}^2 + 6Da\delta_{sc}^4 + Q\pi^2\right), \\ \lambda_2 &= R_{sc}Pm\delta_{sc}^4, \\ \lambda_3 &= QPm^2\delta_{sc}^4\left(\pi^2 + \frac{\pi^4}{Pmq_{sc}\delta_{sc}^2}\right) - \frac{R_{sc}Pmq_{sc}^2}{2}. \end{aligned} \tag{51}$$

Dropping t and y-dependence terms in the Eq. (50), one obtains

$$\frac{d^2A}{dX^2}+\frac{\lambda_2}{\lambda_1}(1-\frac{\lambda_3}{\lambda_1}|A|^2)A=0, \tag{52}$$

$$\therefore A(x)=A_0\tanh(\frac{x}{\Lambda_0}), \tag{53}$$

here

$$A_0=(\lambda_2/\lambda_3)^{\frac{1}{2}} \quad \text{and} \quad \Lambda_0=(2\lambda_1/\lambda_2)^{\frac{1}{2}}.$$

4.1. Heat transport by convection

From Eq. (53), the maximum steady amplitude A is $|A_{max}|$

$$|A_{max}|=\left(\frac{\epsilon^2\lambda_2}{\lambda_3}\right)^{\frac{1}{2}}, \tag{54}$$

The Nusselt number in terms of amplitude A defined as

$$Nu=1+\frac{\epsilon^2}{\delta_{sc}^2}|A_{max}|^2. \tag{55}$$

From Eq. (55), we obtain convection for $R > R_{sc}$ and conduction for $R \leq R_{sc}$. Eq. (50) is valid for $\lambda_3 > 0$ which is possible when $R > R_{sc}$, Thus we get 1. convection for $Nu > 1$ 2. conduction for $Nu \leq 1$ (see in Fig. 6).

5. Results and Discussion

The analytical and numerical results of Double diffusive convection of Maxwell fluid in a horizontal layer with the effect of magnetic field in a porous medium are presented and discussed in this section with graphical representation.

In Fig.1, the neutral curves are presented, illustrating their behavior under various values of Q at the onset of stationary and oscillatory convection. Notably, it is observed that as the value of Q increases, these neutral curves shift upward, indicative of increased stability within the system, thereby highlighting the stabilizing influence of Q. Within the context of magneto-convection, this phenomenon plays a crucial role in monitoring heat transmission. The magnetic field, in this regard, exerts the Lorentz force. When this force remains relatively smaller than the viscous or turbulent pressure, it leads to convective motions that twist and stretch the magnetic field, intensifying flow in turbulent conditions. On the other hand,

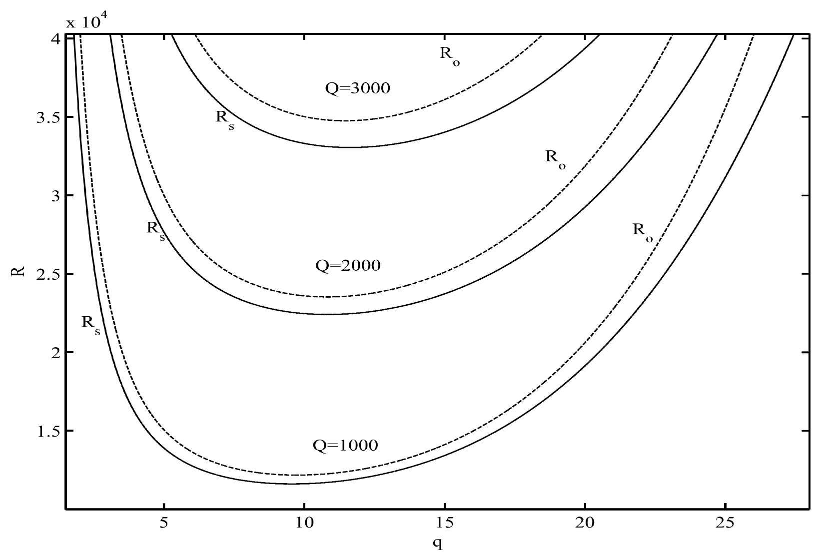

Figure 1: Marginal stability curves for Da = 0.05, λ = 0.5, *Pm* = 0.001.

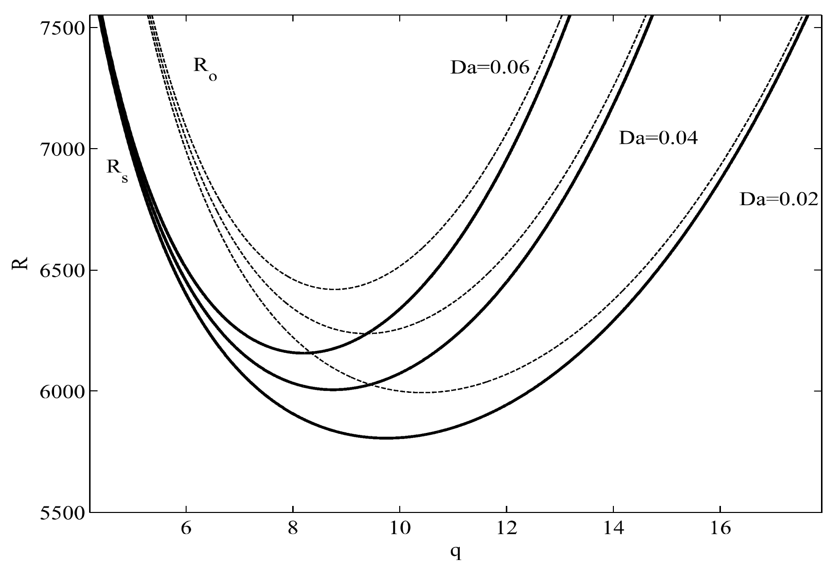

Figure 2: Marginal stability curves for Q = 500, λ = 0.25, *Pm* = 0.0001.

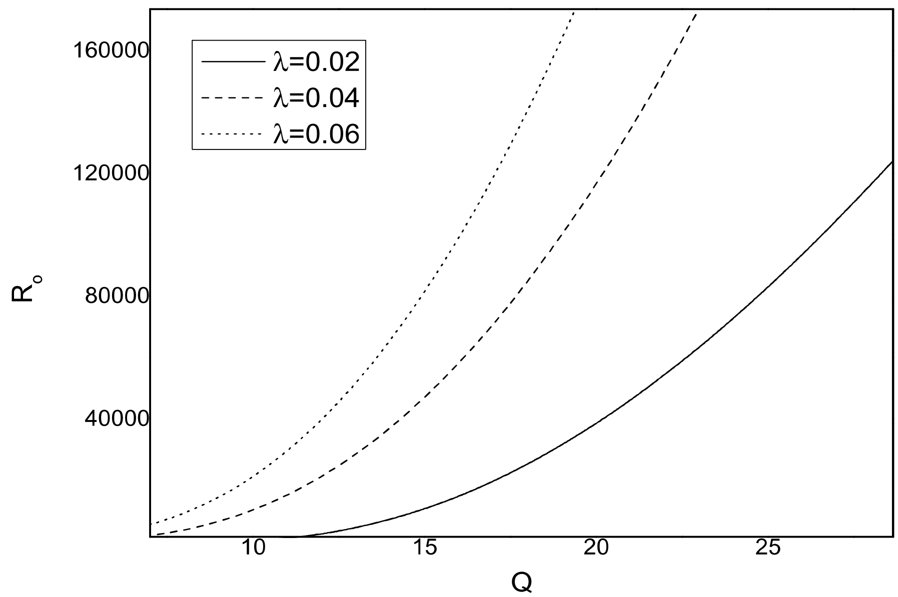

Figure 3: Variation of R_c^O with Q for different values of λ at $Da = 0.001$, $Pm = 0.05$.

when the Lorentz forces overpower the viscous forces or turbulent pressure, the magnetic field effectively channels plasma motions along its direction, inhibiting convective motion. Fig. 2 displays the neutral curves for different values of *Da* at the onset of both convection. In Fig.

2, we observed that Darcy value *Da* decreases with the increase of *Da*, which indicates the existence of Darcy number advances the onset of both convection. This is attributed to the fact that as *Da* increases, the viscous forces present in the system become stronger, which hinders the fluid from moving easily, and hence the system stabilizes.

In Figs. 3 and 4, we represent the variation of the R_c^O with respect to the Chandrasekhar number (Q) for different values of the λ and the magnetic Prandtl number (Pm). From these figures, it has been observed that the R_c^O increases with the Q, indicating that the Q parameter exerts a stabilizing effect on the oscillatory convection phenomenon.

In Fig. 5, we explore the influence of the magnetic Prandtl number (*Pm*) on R_c^O while considering different values of the Chandrasekhar number (*Q*). Notably, from this figure, we deduce that the R_c^O exhibits a non-monotonic behavior concerning the Pm. This nonmonotonic trend suggests that the interplay between magnetic effects and fluid viscosity plays a crucial role in the overall stability behavior of the oscillatory convection process.

In Tables 1, and 2, we present some examples in which steady or oscillatory instability sets in for the constant values of physical parameters. From table 1, we find there exists a threshold $Q^*(\in 26, 27)$ for the Chandrasekhar number, such that, if $Q > Q^*$, then the convection arises via stationary mode. From Table 2, it was found that initially, the stationary convection sets in, and as soon as the value of Da attains a critical value $(\in (0.3, 0.4)),$, the convection ceases to be oscillatory.

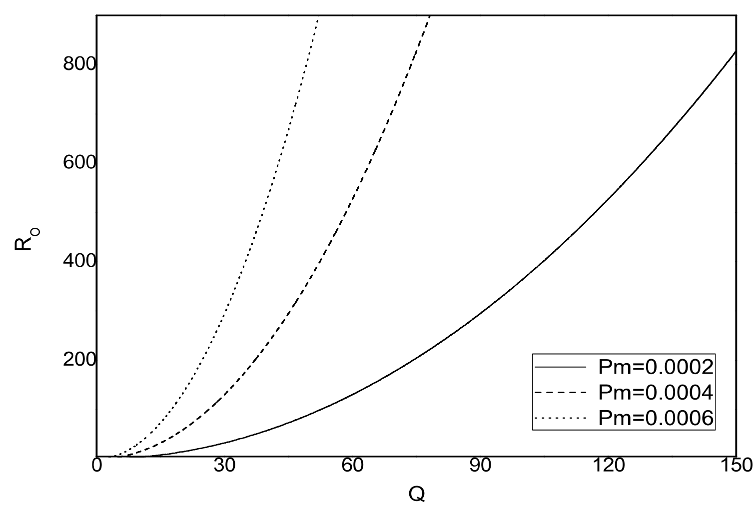

Figure 4: Variation of R_c^O with Q for different values of Pm at $Da = 0.01$, $\lambda = 0.005$.

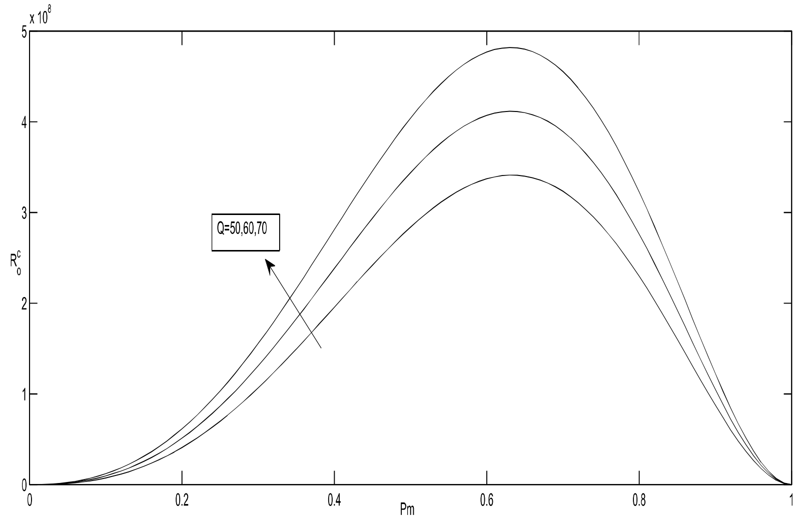

Figure 5: Variation of R_c^O with Pm for different values of Q at $Da = 0.01$, $\Lambda = 0.5$.

Q	Stationary R	Stationary a	Oscillatory R	Oscillatory a	Instability
5	131.50958	4.340971	15.66410	4.340971	Oscillatory
10	203.24061	4.95885	62.11714	4.95885	Oscillatory
15	270.77612	5.37805	138.54948	5.37805	Oscillatory
20	335.97600	5.70067	244.15072	5.70067	Oscillatory
25	399.62746	5.96522	378.10993	5.96522	Oscillatory
26	412.21265	6.012976	408.23325	6.012976	Oscillatory
27	424.75570	6.05933	439.45199	6.05933	Stationary
30	462.15257	6.19062	539.61548	6.19062	Stationary
35	523.80932	6.38765	727.85595	6.38765	Stationary
40	584.76912	6.56315	942.01931	6.56315	Stationary
45	645.15309	6.72174	1181.29417	6.72174	Stationary
50	705.05034	6.86652	1444.86879	6.86652	Stationary

Table 1: Critical stationary and oscillatory Rayleigh numbers for the different values of Q and the fixed values of $\lambda = 0.1$, $Pm = 0.01$, $Da = 0.01$.

Da	Stationary R	Stationary a	Oscillatory R	Oscillatory a	Instability
0	*1205.07624*	*9.95935*	*12947.97019*	*9.95935*	*Stationary*
0.1	*1575.25797*	*5.58617*	*5279.28099*	*5.58617*	*Stationary*
0.2	*1764.19072*	*4.94909*	*3298.03299*	*4.94909*	*Stationary*
0.3	*1916.38818*	*4.60152*	*2396.15263*	*4.60152*	*Stationary*
0.4	*2050.05493*	*4.36725*	*1881.16634*	*4.36725*	*Oscillatory*
0.5	*2172.15751*	*4.19296*	*1548.24596*	*4.19296*	*Oscillatory*
0.6	*2286.22704*	*4.05552*	*1315.38899*	*4.05552*	*Oscillatory*
0.7	*2394.33170*	*3.94285*	*1143.39150*	*3.94285*	*Oscillatory*
0.8	*2497.80185*	*3.84804*	*1011.16266*	*3.84804*	*Oscillatory*
0.9	*2597.55356*	*3.76647*	*906.33551*	*3.76647*	*Oscillatory*
1	*2694.24905*	*3.69528*	*821.20101*	*3.69528*	*Oscillatory*

Table 2: Critical stationary and oscillatory Rayleigh numbers for the different values of Q and the fixed values of $\lambda = 0.01$, $Pm = 0.001$, $Q = 100$.

	$\lambda = 0.01$		$\lambda = 0.03$		$\lambda = 0.05$	
Q	R_o	R_{oc}	R_o	R_{oc}	R_o	R_{oc}
0.5	*5762.53403*	*3.50825*	*10636.39361*	*6.94266*	*26376.80265*	*6.94266*
1.5	*5635.45441*	*13.90335*	*10430.52900*	*27.56209*	*26021.73595*	*27.56209*
2.5	*5516.08971*	*31.21939*	*10238.35287*	*61.99760*	*25699.69476*	*61.99760*
3.5	*5368.05231*	*65.13167*	*10001.91141*	*129.64444*	*25318.76094*	*129.64444*
4.5	*5264.75889*	*98.72785*	*9838.40797*	*196.86140*	*25067.45655*	*196.86140*
5.5	*5167.62667*	*139.35760*	*9685.96711*	*278.36299*	*24844.15644*	*278.36299*
6.5	*5047.04313*	*204.53031*	*9498.81542*	*409.49904*	*24587.97173*	*409.49904*
7.5	*4962.85040*	*261.70310*	*9369.77569*	*524.88794*	*24425.66497*	*524.88794*
8.5	*4883.65884*	*326.02240*	*9249.85562*	*655.04084*	*24287.93000*	*655.04084*
9.5	*4809.17937*	*397.52225*	*9138.57495*	*800.10370*	*24173.98561*	*800.10370*
10.5	*4739.14568*	*476.23672*	*9035.49323*	*960.22349*	*24083.15072*	*960.22349*
11.5	*4652.26137*	*592.47111*	*8910.11112*	*1197.39431*	*23996.98296*	*1197.39431*
12.5	*4591.67850*	*688.15256*	*8824.64538*	*1393.22412*	*23957.93672*	*1393.22412*
13.5	*4516.62025*	*827.13384*	*8721.48891*	*1678.55197*	*23939.23952*	*1678.55197*
14.5	*4464.37401*	*939.96879*	*8651.83108*	*1910.91042*	*23949.85139*	*1910.91042*
15.5	*4415.40634*	*1060.21251*	*8588.47743*	*2159.17785*	*23981.33449*	*2159.17785*
16.5	*4354.94456*	*1232.12174*	*8513.38439*	*2515.21444*	*24055.54118*	*2515.21444*
17.5	*4313.03177*	*1369.78660*	*8463.80596*	*2801.20290*	*24135.28664*	*2801.20290*
18.5	*4273.91350*	*1514.97522*	*8419.77755*	*3103.61723*	*24235.69200*	*3103.61723*
19.5	*4237.46631*	*1667.72221*	*8381.11236*	*3422.61482*	*24356.83878*	*3422.61482*
20.5	*4192.82789*	*1883.20226*	*8337.60833*	*3874.01517*	*24550.89617*	*3874.01517*

Table 3: Stationary and critical stationary Rayleigh numbers for the different values of λ and the fixed values of $Pm = 0.002$ and $Da = 0.01$.

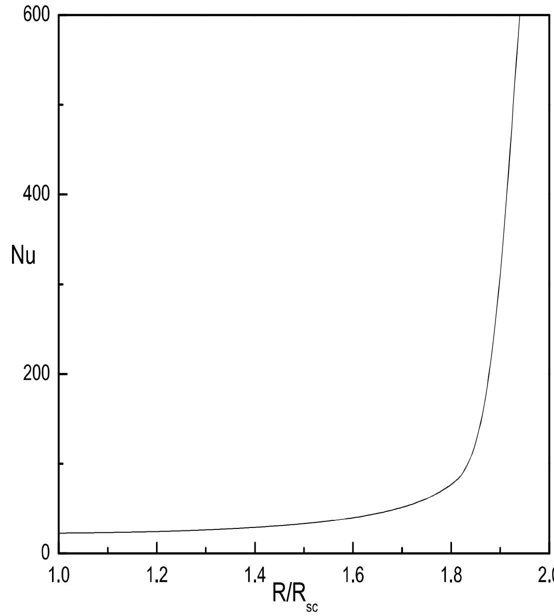

Figure 6: The Figure is plotted for the fixed values of $Q = 1000$, $Pm = 0.001$, $Da = 0.1$.

	$Pm = 0.0005$		$Pm = 0.001$		$Pm = 0.0015$	
Q	R_o	R_{oc}	R_o	R_{oc}	R_o	R_{oc}
0.5	887.22072	0.29697	3691.35946	1.18857	8640.32999	2.67582
1.5	871.62639	1.82234	3626.66806	7.30264	8489.37797	16.46089
2.5	857.16755	4.64803	3566.70131	18.64922	8349.48537	42.08955
3.5	839.53630	10.44675	3493.60044	41.98489	8179.00995	94.91343
4.5	827.46776	16.32543	3443.58163	65.69270	8062.40882	148.69388
5.5	816.32690	23.52065	3397.42467	94.76387	7954.85205	214.76356
6.5	802.82881	35.17068	3341.52968	141.93716	7824.67232	322.20854
7.5	793.66382	45.45688	3303.60055	183.67777	7736.39100	417.48461
8.5	785.27501	57.07599	3268.90471	230.91508	7655.68709	525.50832
9.5	777.62545	70.03294	3237.28897	283.68960	7582.20335	646.41973
10.5	768.51830	89.39852	3199.68689	362.73946	7494.89910	827.92684
11.5	764.41259	99.98019	3182.75296	406.01336	7455.62623	927.47196
12.5	757.05638	122.94866	3152.45144	500.12015	7385.44799	1144.35852
13.5	750.79212	148.33387	3126.70519	604.38761	7325.96140	1385.26055
14.5	746.77918	168.96590	3110.25533	689.31567	7288.06164	1581.90636
15.5	743.33192	190.96907	3096.16717	780.05683	7255.70969	1792.40281
16.5	739.58562	222.44821	3080.93349	910.16080	7220.91798	2094.86498
17.5	737.39353	247.67034	3072.08913	1014.63077	7200.89248	2338.26068
18.5	735.71574	274.28047	3065.39497	1125.05575	7185.92512	2596.01047
19.5	734.54035	302.28371	3060.80217	1241.47885	7175.90332	2868.26799
20.5	733.73678	341.79725	3057.87404	1406.11500	7170.06598	3254.11359

Table 4: Stationary and critical stationary Rayleigh numbers for the different values of Pm and the fixed values of $\lambda = 0.04$ and $Da = 0.01$.

6. Conclusion

In this study, the magneto convection in a Maxwell fluid due to a vertical magnetic field saturated porous medium is analyzed. For modeling the fluid flow, the Brinkman equation and the Oberbeck-Boussinesq approximation are adopted for modeling. The problem was studied by performing both linear and weakly nonlinear analyses analytical methods. The normal mode method has been employed to solve the governing equations. The critical stationary and oscillatory Rayleigh numbers versus wave numbers are plotted and discussed.

The behavior of various parameters, like the Q,Λ, Da, and Pm, has been analyzed. The main findings of the analysis are as follows:

- It is obtained that the Chandrasekhar number and Darcy number have a stabilizing effect on the system. Also, it is found that the Critical oscillatory Rayleigh number is a non-monotonic function of Pm.
- From the results, to study the heat transport by convection, we have derived the amplitude equation. A multiple-scale analysis is used to derive the amplitude equation.
- The relationship between the governing parameters (Q and Pm) and the ROc offers valuable physical insights into the intricate nature of oscillatory convection phenomena in the system under investigation.

In future work, we plan to study linear instability numerically and extend our investigations to solve the nonlinear stability using the Energy method. Additionally, we aim to explore the interplay between linear and nonlinear effects to gain a comprehensive understanding of the system's stability behavior.

References

[1] Alfven, Hannes. "Discussion of the origin of the terrestrial and solar magnetic fields." Tellus 2, no. 2, 74-82, (1950).

[2] Thompson, W. B. "CXLIII. Thermal convection in a magnetic field." The London, Edinburgh, and Dublin Philosophical Magazine and Journal of Science 42, no. 335, 1417-1432, (1951).

[3] Chandrasekhar, S., Hydrodynamic and hydromagnetic stability. Oxford: Oxford University press (1961).

[4] Sparrow, E. M., and R. D. Cess. "The effect of a magnetic field on free convection heat transfer." International Journal of Heat and Mass Transfer 3, no. 4, 267-274, (1961).

[5] Nield, D. A. "Onset of thermohaline convection in a porous medium." Water Resources Research 4, no. 3, 553-560, (1968).

[6] Taunton, J. W., E. N. Lightfoot, and Theodore Green. "Thermohaline instability and salt fingers in a porous medium." The Physics of Fluids 15, no. 5, 748-753, (1972).

[7] Knobloch, E., N. O. Weiss, and L. N. Da Costa. "Oscillatory and steady convection in a magnetic field." Journal of Fluid Mechanics 113, 153-186, (1981).

[8] Rudraiah, N., P. Kn Srimani, and R. Friedrich. "Finite amplitude convection in a twocomponent fluid saturated porous layer." International Journal of Heat and Mass Transfer 25, no. 5, 715-722, (1982).

[9] Poulikakos, Dimos. "Double diffusive convection in a horizontal sparcely packed porous layer." International communications in heat and mass transfer 13, no. 5 , 587-598, (1986).

[10] Maxwell, J.C., IV. On the dynamical theory of gases. Philosophical transactions of the Royal Society of London, (157), 49-88, (1987).

[11] Malashetty, M. S. "Anisotropic thermoconvective effects on the onset of double diffusive convection in a porous medium." International journal of heat and mass transfer 36, no. 9, 2397-2401, (1993).

[12] Kalla, L., P. Vasseur, R. Benacer, H. Beji, and R. Duval. "Double diffusive convection within a horizontal porous layer salted from the bottom and heated horizontally." International communications in heat and mass transfer 28, no. 1, 1-10, (2001).

[13] Ingham, D.B. and Pop, I. eds., Transport phenomena in porous media III (Vol. 3). Elsevier, (2005).

[14] Uetake, Hiromichi, Noriyuki Hirota, Jun Nakagawa, Yasuhiro Ikezoe, and Koichi Kitazawa. "Thermal convection control by gradient magnetic field." Journal of Applied Physics 87, no. 9, 6310-6312, (2000).

[15] Khuzhayorov, B., Auriault, J.L. and Royer, P., Derivation of macroscopic filtration law for transient linear viscoelastic fluid flow in porous media. International Journal of Engineering Science, 38(5), 487-504, (2000).

[16] Sharma, R.C., The effect of magnetic field dependent viscosity on thermosolutal convection in a ferromagnetic fluid saturating a porous medium. Transport in Porous Media, 60(3), pp.251-274, (2005).

[17] Nield, Donald A., and Adrian Bejan. Convection in porous media. Vol. 3. New York: springer, (2006).

[18] Abbas, Z., Sajid, M. and Hayat, T., MHD boundary-layer flow of an upper-convected Maxwell fluid in a porous channel. Theoretical and Computational Fluid Dynamics, 20(4), 229-238, (2006).

[19] Hayat, T., Abbas, Z. and Sajid, M., Series solution for the upper-convected Maxwell fluid over a porous stretching plate. Physics Letters A, 358(5-6), 396-403, (2006).

[20] Hayat, T., Sajjad, R., Abbas, Z., Sajid, M. and Hendi, A.A., Radiation effects on MHD flow of Maxwell fluid in a channel with porous medium. International Journal of Heat and Mass Transfer, 54(4), 854-862, (2011).

[21] Gaikwad, S. N., and M. Dhanraj. ”Onset of double diffusive convection in a Maxwell fluid saturated anisotropic porous layer with internal heat source.” Special Topics and Reviews in Porous Media: An International Journal 4, no. 4, (2013).

[22] Vad´asz, Peter, ed. ”Emerging topics in heat and mass transfer in porous media: From bioengineering and microelectronics to nanotechnology.” (2008).

[23] Ghosh, S. K., O. Anwar B´eg, and J. Zueco. ”Hydromagnetic free convection flow with induced magnetic field effects.” Meccanica 45, no. 2, 175-185, (2010).

[24] Wang, S. and Tan, W., Stability analysis of soret-driven double-diffusive convection of Maxwell fluid in a porous medium. International Journal of Heat and Fluid Flow, 32(1), 88-94, (2011).

[25] Malashetty, M.S. and Biradar, B.S., The onset of double diffusive convection in a binary Maxwell fluid saturated porous layer with cross-diffusion effects. Physics of Fluids, 23(6), 064109, (2011).

[26] Babu, A. B., Reddy, G. S. K., & Tagare, S. G. . Nonlinear magneto convection due to horizontal magnetic field and vertical axis of rotation due to thermal and compositional buoyancy. Results in Physics, 12, 2078-2090, (2019).

[27] Benerji Babu, A., Reddy, G. S. K., & Tagare, S. G. . Nonlinear magnetoconvection in a rotating fluid due to thermal and compositional buoyancy with anisotropic diffusivities. Heat Transfer—Asian Research, 49(1), 335-355, (2020).

[28] Reddy, Gundlapally Shiva Kumar, Nilam Venkata Koteswararao, Ragoju Ravi, Kiran Kumar Paidipati, and Christophe Chesneau. "Dissolution-Driven Convection in a Porous Medium Due to Vertical Axis of Rotation and Magnetic Field." Mathematical and Computational Applications 27, no. 3, 53, (2022).

[29] Raghunatha, K.R., Shivakumara, I.S. and Shankar, B.M., Weakly nonlinear stability analysis of triple diffusive convection in a Maxwell fluid saturated porous layer. Applied Mathematics and Mechanics, 39(2), 153-168, (2018).

[30] Karimi, M., Khosravi, M., Fathollahi, R., Khandakar, A., and Vaferi, B. . Determination of the heat capacity of cellulosic biosamples employing diverse machine learning approaches. Energy Science and Engineering, (2022).

[31] Rastegarpouyani, H., Mohebbi, S. R., Hosseini, S. M., Azimzadeh, P., Sharifian, A., Asadzadeh-Aghdaei, H., ... and Zali, M. R. Detection of Parvovirus 4 in Iranian patients with HBV, HCV, HIV mono-infection, HIV and HCV co-infection.Gastroenterology and Hepatology From bed to Bench, 11(2), 138, (2018) .

[32] Hosseinzadeh, K., Gholinia, M., Jafari, B., Ghanbarpour, A., Olfian, H. and Ganji, D.D., Nonlinear thermal radiation and chemical reaction effects on Maxwell fluid flow with convectively heated plate in a porous medium. Heat Transfer—Asian Research, 48(2), 744-759, (2019).

[33] Jahanmahin, O., Rahmati, M. M. M., Mohammadi, T., Babaee, J., and Khosravi, A. Cr (VI) ion removal from artificial waste water using supported liquid membrane. Chemical Papers, 70(7), 913-925, (2016).

[34] Pasha, P., Mirzaei, S., and Zarinfar, M. Application of numerical methods in micropolar fluid flow and heat

transfer in permeable plates. Alexandria Engineering Journal, 61(4), 2663-2672, (2022).

[35] Fathollahi, R., Hesaraki, S., Bostani, A., Shahriyari, E., Shafiee, H., Pasha, P., and Ganji, D. D. Applying numerical and computational methods to investigate the changes in the fluid parameters of the fluid passing over fins of different shapes with the finite element method. International Journal of Thermofluids, 15, 100187, (2022).

[36] Faress, F., Yari, A., Rajabi Kouchi, F., Safari Nezhad, A., Hadizadeh, A., Sharif Bakhtiar, L., and Mahmoudi, N. Developing an accurate empirical correlation for predicting anti-cancer drugs' dissolution in supercritical carbon dioxide. Scientific Reports, 12(1), 1-17, (2022).

[37] Charchi, N., Li, Y., Huber, M., Kwizera, E. A., Huang, X., Argyropoulos, C.,and Hoang, T. Small mode volume plasmonic film-coupled nanostar resonators. Nanoscale advances, 2(6), 2397-2403, (2020).

[38] Abdollahzadeh, M. J., Fathollahi, R., Pasha, P., Mahmoudi, M., Samimi Behbahan, A., and Domiri Ganji, D. Surveying the hybrid of radiation and magnetic parameters on Maxwell liquid with TiO2 nanotube influence of different blades. Heat Transfer, 51(6),4858-4881, (2022).

[39] Reddy, G.S.K. and Ragoju, R., Thermal instability of a maxwell fluid saturated porous layer with chemical reaction. Special Topics and Reviews in Porous Media: An International Journal, 13(1), (2022).

[40] Ragoju, R., & Shekhar, S. Linear and Weakly Nonlinear Analyses of Magneto- Convection in a Sparsely Packed Porous Medium under Gravity Modulation. Journal of Applied Fluid Mechanics, 13(6), 1937-1947, (2020).

[41] Babu, A. B., Ravi, R., & Tagare, S. . Nonlinear thermohaline magnetoconvection in a sparsely packed porous medium. Journal of Porous Media, 17(1), (2014).

[42] Shadman, P., Parhizi, Z., Fathollahi, R., Zarinfar, M., Anisimova, E. Y., and Pasha, P. Combined septum and chamfer fins on threated stretching surface under the influence of nanofluid and the magnetic parameters for rotary seals in computer hardware. Alexandria Engineering Journal, 62, 489-507, (2023).